Bolt Beranek and Newman Inc.

Report No. 4413

ANALYSIS OF SELECTED TOPICS IN THE METHODOLOGY OF THE INTEGRATED NOISE MODEL

Kenneth M. Eldred
Robert L. Miller

November 1980

Prepared for:

U.S. Department of Transportation
Transportation Systems Center
Cambridge, MA 02142

Report No. DOT-TSC-1782

ANALYSIS OF SELECTED TOPICS IN THE METHODOLOGY OF THE INTEGRATED NOISE MODEL

Kenneth M. Eldred
Robert L. Miller

BOLT BERANEK AND NEWMAN INC.
50 Moulton Street
Cambridge, MA 02238

November 1980

FINAL REPORT

Document is available to the U.S. public through the
National Technical Information Service,
Springfield, Virginia 22161

Prepared for
U.S. DEPARTMENT OF TRANSPORTATION
Transportation Systems Center
Cambridge, MA 02142

Technical Report Documentation Page

1. Report No.	2. Government Accession No.	3. Recipient's Catalog No.
DOT-TSC-1782		

4. Title and Subtitle	5. Report Date
Analysis of Selected Topics in the Methodology of the Integrated Noise Model	November 1980
	6. Performing Organization Code
7. Author(s)	8. Performing Organization Report No.
Kenneth M. Eldred & Robert L. Miller	BBN Report No. 4413
9. Performing Organization Name and Address	10. Work Unit No. (TRAIS)
Bolt Beranek and Newman Inc. 50 Moulton Street Cambridge, Massachusetts 02238	FA165/R1105
	11. Contract or Grant No.
	DOT-TSC-1782
12. Sponsoring Agency Name and Address	13. Type of Report and Period Covered
U.S. Department of Transportation Transportation Systems Center Cambridge, MA 02142	Final November 1980
	14. Sponsoring Agency Code

15. Supplementary Notes

16. Abstract

This report reviews the Integrated Noise Model (INM) general methodology for determining the nearest segment and the transition algorithms, gives examples of anomalous errors associated with the current methodology and provides recommendations for changes to the methodology so that these errors are minimized. It also examines the special case of the noise at the beginning of takeoff roll, and provides new noise data and recommended algorithms for improving the description of this special situation.

17. Key Words	18. Distribution Statement
airport noise, noise model, aircraft noise	

19. Security Classif. (of this report)	20. Security Classif. (of this page)	21. No. of Pages	22. Price

TABLE OF CONTENTS

LIST OF FIGURES

List of Figures *(cont.)*

1. INTRODUCTION

The Integrated Noise Model (INM) specifies the location of an aircraft relative to an observer by a set of ground tracks underneath the flight path and by a profile of height above airport and other operating parameters. Each ground track is specified in terms of straight and circular segments. To determine the noise contribution of a specific aircraft flight (i.e., a flight is aircraft type times equivalent operations for a specific track), the program determines the point on the ground track that is closest to the observation location. It then computes the distance from the beginning of the ground track to this nearest point on the track, and determines the height above airport, the power setting and the velocity of the aircraft at this point. The program then computes the slant distance between the observation location and the aircraft, and the noise contribution associated with the aircraft type, power setting, velocity and slant distance.

This methodology is rigorously correct for a straight horizontal flight path of infinite length, an assumption that is inherent in the program's noise data file. Also, the error in noise energy is less than 3% if a straight path segment extends for ± 70° relative to the perpendicular from the observer to the track, and less than 20% for a segment extending ± 45°. For the majority of observer locations at an airport with simple track geometries that are primarily outgoing from the airport, these conditions frequently occur, and errors resulting from this methodology are negligible. However, for curved tracks and more complex geometry where noise from more than one segment affects an observation location the error may be significant.

Additionally, the methodology is susceptible to large changes in noise level over a small change of distance in the vicinity of certain observer locations. These large changes in noise occur when a small change in observer position results in a shift to a new closest track segment which is considerably removed from the original segment as measured in distance along the track. Such a change along the track may involve skipping several track segments and result in significant differences in aircraft height above ground, power setting, velocity, and elevation angle – all of which affect the noise contribution.

Large changes in noise contribution for small changes in observer position may become discontinuities, particularly in the vicinity of the center of a circular turn or along a bisector of two straight line tracks. Because the INM gradient method for developing a series of points along a specified noise contour fails when it encounters a discontinuity, the INM contains several algorithms that are designed to ensure that no actual discontinuity exists. These transition algorithms fulfil their intended purpose, i.e., to enable the program to function, but they do not resolve the errors that may exist in the noise calculations.

Finally, the INM contains a default mode for the special case of the beginning of takeoff roll that results in the output of a semi-circular contour which overstates the noise, particularly directly behind the aircraft. This overstatement is not significant when landings occur in this region, but for cases dominated by takeoff, the errors may be significant.

This report reviews the INM general methodology for determining the nearest segment and the transition algorithms, gives examples of anomalous errors associated with the current methodology and provides recommendations for changes to the methodology so that these

errors are minimized. It also examines the special case of the noise at the beginning of takeoff roll, and provides new noise data and recommended algorithms for improving the description of this special situation.

2. INM METHODOLOGY FOR DEFINING AIRCRAFT POSITION ON FLIGHT TRACK AND FOR ELIMINATING DISCONTINUITIES

The INM contains three subroutines that govern the determination of aircraft position on a flight track with respect to observer position and provide for eliminating potential discontinuities in noise. These subroutines are:

- STRAIT – computes the distance from an observer location to a straight line segment of a given ground track.
- CURVE – computes the shortest distance from an observer location to a specified circular segment on a given ground track and provides a partial noise correction for the increase of duration for observer locations on the inside of a turn.
- HBT – determines shortest distance to ground track, and the track segment in which it occurs, distance along track to point of closest approach, identifies a secondary segment (if any) that contains the next nearest point of approach, and provides for transition algorithms between primary and secondary segments for computation of noise expsosure.

The following subsections taken primarily from reference (1) provide a description of the functioning of these three subroutines.

STRAIT

STRAIT computes the distance (d) between a specified observation point (P) and a specific straight ground track segment, and the distance (x) between the beginning of the segment and the intersection of the perpendicular to the segment through P.

Figure 1 illustrates this geometry and the limitations in the unshaded region in which P must lie for the calculation of d and x to be completed:

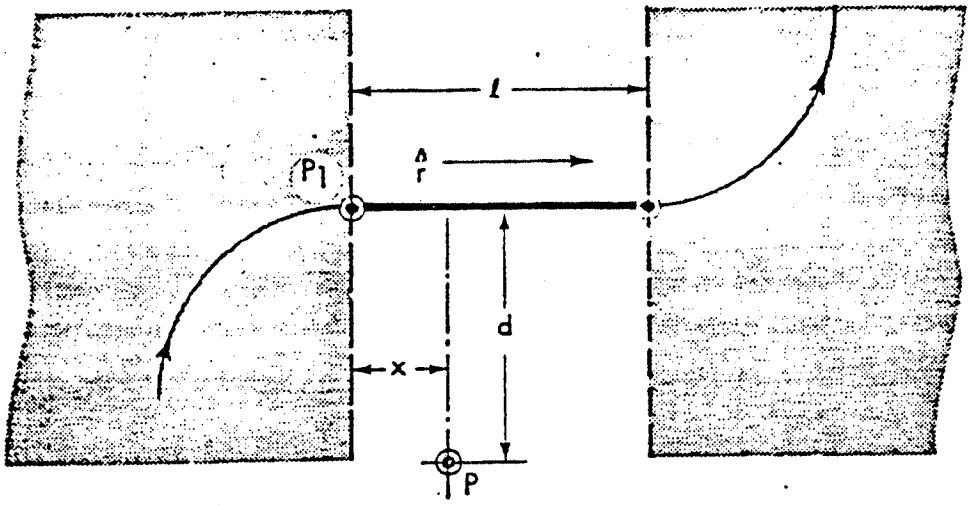

FIGURE 1: GROUND TRACK GEOMETRY FOR STRAIT.

The processing performed by STRAIT is summarized in the following steps:

1) Define:

$$x = \overrightarrow{P_1 P} \cdot \hat{r} \quad \text{(vector dot product)}$$

where $\overrightarrow{P_1 P}$ is the vector from P_1 to P and x is the distance along the segment.

2) Point P lies within the unshaded allowable region if and only if

$$0 < x < \ell \quad .$$

3) If point P lies outside the allowable region it is deemed to be outside the range of the segment and this result is returned to the calling program.

4) If P lies within the allowable region, the perpendicular distance to the segment d, is calculated by:

$$d = \sqrt{|\overrightarrow{P_1P}|^2 - x^2}$$

and the values of x and d are returned to the calling program.

CURVE

CURVE computes the shortest distance (d) from a specified observation point (P) to a specified ground track circular segment, and computes a correction (DB) to the noise level, when the point is on the inside of a turn. Figure 2 illustrates the geometry for CURVE and the limitations on the unshaded region in which P must lie for the calculations to be completed.

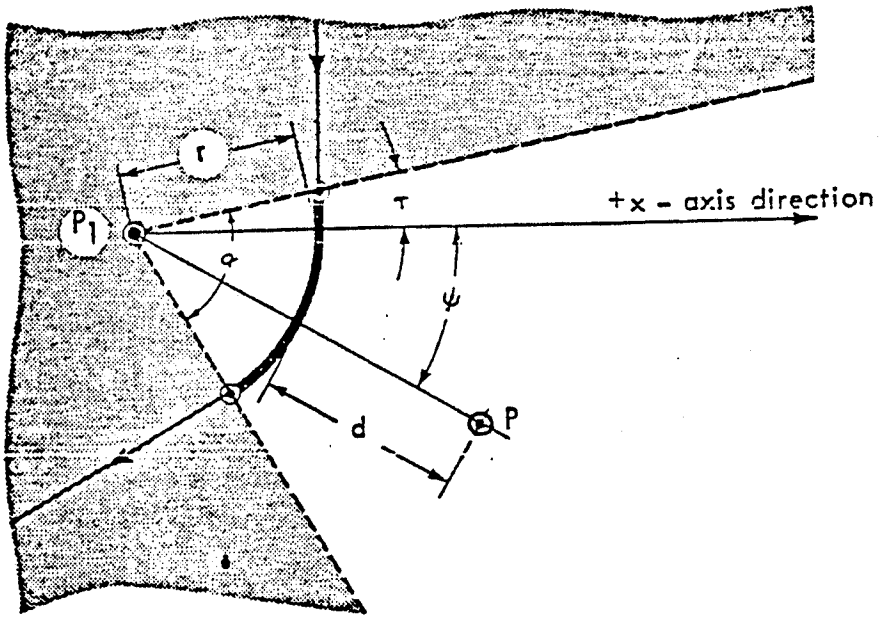

FIGURE 2: GROUND TRACK GEOMETRY FOR CURVE.

The processing performed by CURVE is summarized in the following steps:

1) Compute ψ, the angle between P_1P and the positive x-direction, such that ψ is in the range $-\pi$ to π.

2) The point P lies within the unshaded allowable region if and only if one and only one of the following is true:

$$0 < (\psi - \tau)S < \alpha$$

or

$$(\psi - \tau)S + 2\pi < \alpha$$

where $-\pi \leq \tau \leq \pi$, $0 < \alpha < 2\pi$ and $S = -1, +1$ for right and left turns, respectively, when tracing the track from the runway outward.

3) If point P lies outside the allowable region it is deemed to be outside the range of the segment and this result is returned to the calling program.

4) If P is in the unshaded sector calculate the shortest distance to the ground track segment and the distance along the segment.

   a) The shortest distance (d) to the segment is calculated by

$$d = \left| \left| \overrightarrow{P_1P} \right| - r \right|$$

b) The distance (TAU) along the circular segment from its beginning to the point that is closest to point P is given by

$$TAU = \left|(\psi - \tau)r\right|$$

c) The values of d and TAU are returned to the calling program.

5) If the point P lies in the allowable region and if it also lies inside the circular ground track segment, a noise correction (DB) is computed

a) P lies inside the circular segment if:

$$\overrightarrow{P_1P} - r < 0$$

b) If P lies outside the circular segment the value of the correction (DB) is zero and is returned to the calling program.

c) If P lies inside the circular segment the correction (DB) is specified for three angular regions as follows:

$$DB = \frac{d}{r} Y\left[\frac{5\Phi}{\alpha}\right] \qquad \text{for } \frac{\Phi}{\alpha} < .2$$

$$DB = \frac{d}{r} Y \qquad \text{for } .2 \leq \frac{\Phi}{\alpha} \leq .8$$

$$DB = \frac{d}{r} Y \left[5\left(1 - \frac{\Phi}{\alpha}\right)\right] \qquad \text{for } \frac{\Phi}{\alpha} > .8$$

where $Y = 3$, when $\frac{6\alpha}{\pi} \geq 3$

$= \frac{6\alpha}{\pi}$, when $\frac{6\alpha}{\pi} < 3$

and $\Phi = |\psi - \tau|$ the angular displacement of the point from the beginning of the circular segment. The value of DB is returned to the calling program.

The correction (DB) provides a maximum increase of 3 dB to the noise contribution when the observation point is at the center of the circular ground track segment and the angle of the turn equals or exceeds $\pi/2$. The magnitude of the correction in decibels is directly proportional to d/r, becoming zero when the observation point is on the circular ground track segment. The correction provides for transition regions at the beginning and end of the circular segment each of which extends for 1/5 of the segment.

HBT

HBT computes the shortest distance from a specified observation point to a specified ground track, the track segment associated with the shortest distance, and the distance along the track from its beginning to the point of closest approach. It also computes similar quantitites for a secondary segment which has the next shortest distance, if it exists, and provides for a smooth transition in the value of the noise in regions where more than one segment can contribute to its value.

The shortest distance(s) from an observation point to the segment(s) of a specified ground track and the distance to the point of closest approach on the segment are computed for HBT by STRAIT or CURVE, as appropriate. The distance along the track from its beginning to the point of closest approach is computed in HBT by adding the lengths of all prior segments to the distance computed along the segment associated with the point of closest approach.

When an observation point is found to be in the allowable region of two or more segments HBT determines the closest segment (Max 1) and the next to closest segment (Max 2). It then computes

corrections in the general manner described in the following steps, as appropriate.

1) Determine the difference (D) in the distances (S_1 and S_2) to the nearest segment (Max 1) and the next nearest segment (Max 2)

$$D = S_2 - S_1$$

2) Define DM equal to the length of the shortest straight segment on the track, or 1/2 the smallest turn radius, wheichever is less.

3) If ($D \geq DM$) use the nearest segment (Max 1) for all parameters, ignoring all other segments.

4) If ($D < DM$) and if there are two or more segments separating Max 1 and Max 2, or one segment if both Max 1 and Max 2 are curved segments, then the decibel corrections to be added arithmetically to the noise are:

DA = 0, the correction for noise computed from Max 1,

and

DB = $-20 \cdot G(D)$, the correction for noise computed for Max 2

where $G(D) = (D/DM)^2$.

This algorithm provides a smooth transition in noise through a region between the two segments of width equal to 2 DM. At the edge of the region towards Max 1, $D/DM = 1$ and the noise from Max 2 is attenuated by 20 decibels and that from Max 1 by zero decibels. At the center of the region, $D/DM = 0$ and the noise

from Max 2 has zero attenuation as does the noise from Max 1. Thus, at the edge of the transition zone the noise level is essentially that associated with the nearest segment (Max 1), the level from the secondary segment makes a negligible addition, having been attenuated 20 dB. However, at the middle of the transition zone where the distances to the two segments are equal neither noise level is attenuated so that they add together to their full combined value on an energy basis. See Figure 3 for additional details.

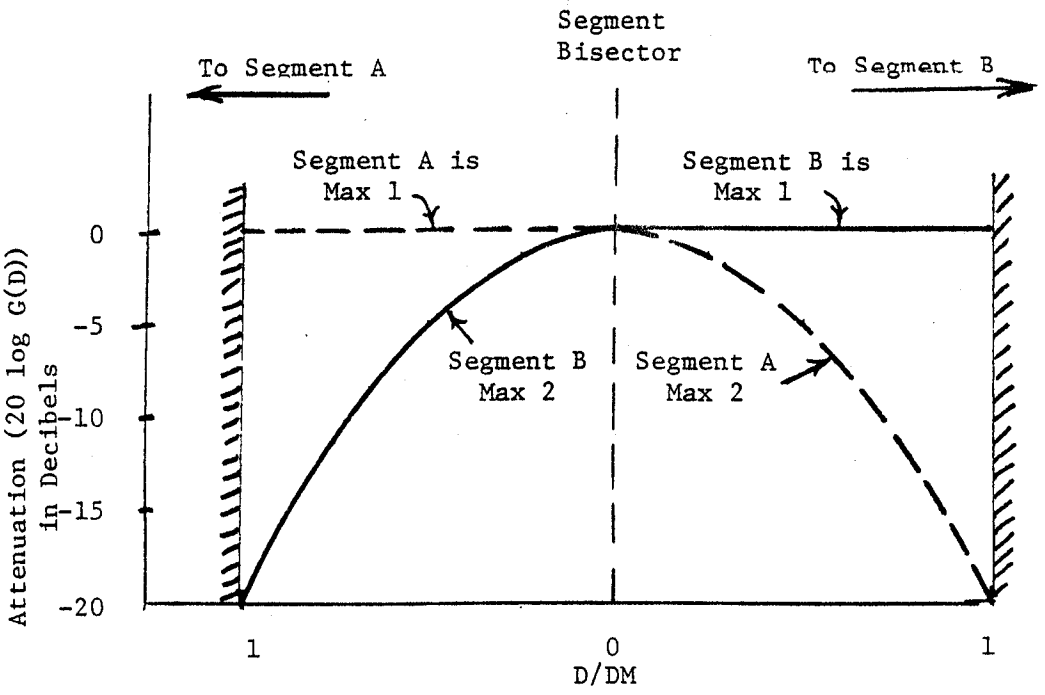

FIGURE 3: ILLUSTRATION OF THE TRANSITION ALGORITHM FOR THE NOISE AT OBSERVATION LOCATIONS WITHIN THE RANGE OF TWO STRAIGHT GROUND TRACK SEGMENTS.

HBT contains several additional algorithms which provide necessary transitions between straight and circular paths. They operate in essentially the same manner, as that discussed above, but are somewhat more complex to prevent possible discontinuities associated with the noise corrections in CURVE which were designed to approximate the effects of duration on the inside of circular segments.

3. DISCUSSION OF ANOMOLIES RESULTING FROM THE EXISTING GENERAL METHODOLOGY

The INM methodology is based primarily on defining the noise received at an observation location from an aircraft at the closest point of approach on its ground track. The principal weakness of this methodology is that the point of closest approach on a ground track may not be associated with the maximum noise received at the observation location because of one or more of several reasons:

- The point of closest approach on the ground track is not related to the point of closest approach on the three dimensional flight path.
- The aircraft thrust setting, and hence noise, may be greater at a more distant location on the flight path.
- Ground attenuation and related angle of elevation effects may reduce the noise received from the closest ground track segment relative to that received from a more distant location on the flight path.
- For complex geometrical flight paths the noise received at an observation location may have significant contributions from several flight path segments, not just one.

Figure 4 provides one example of the deficiency that can result in serious distortion of the contours. The example shows a single runway operation with a flight track designed to bring the aircraft back over the airport after climbing out over water. This simplified example had 500 daily takeoff operations of 727-100 aircraft which climbed to over 8000 ft. altitude when crossing the airport. The contours exhibit a wedge shaped void

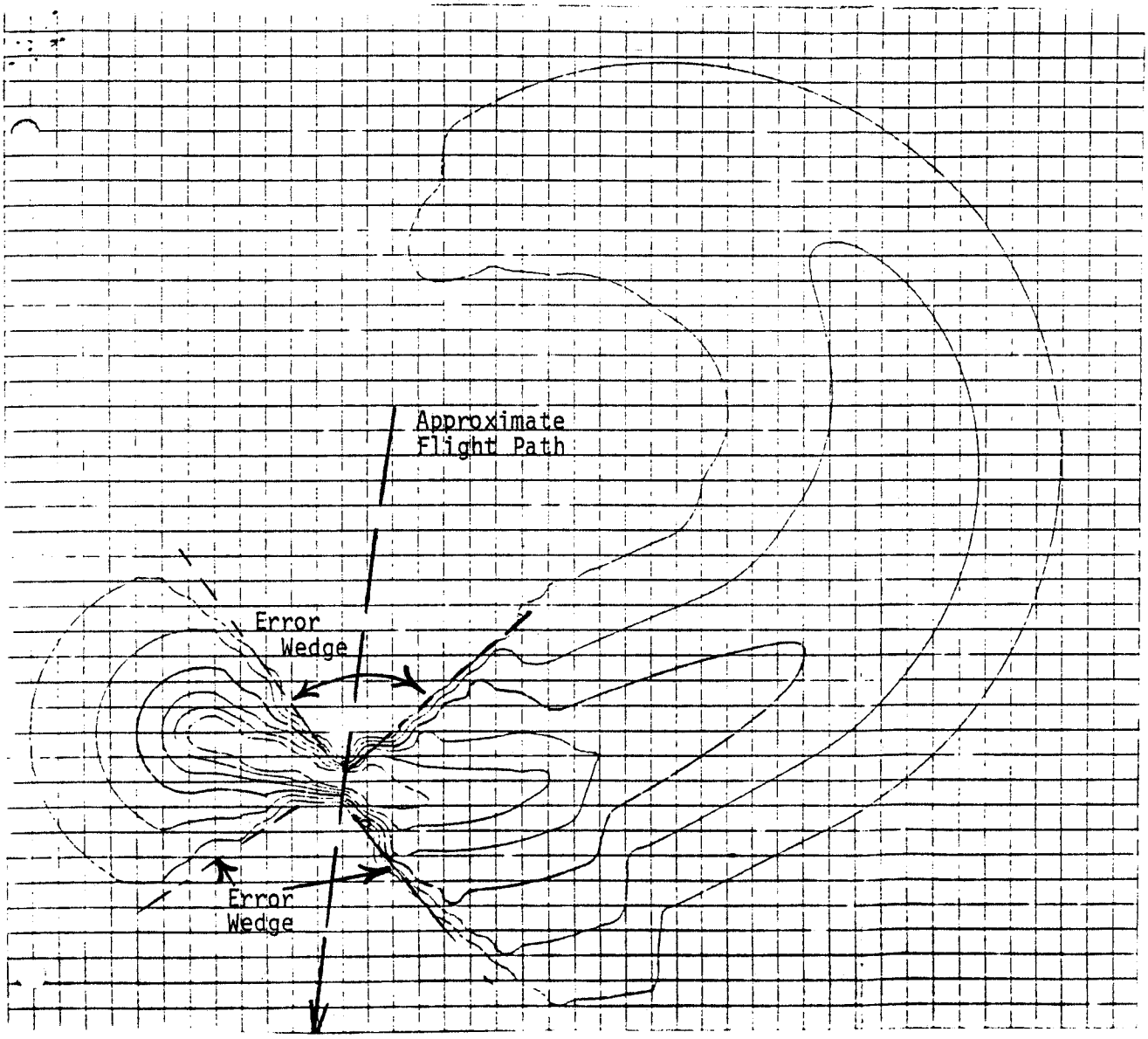

FIGURE 4: EXAMPLE OF THE ERROR PRODUCED WHEN IN THE INM A FLIGHT PATH CROSSES ITSELF, RESULTING IN AN INTERACTION OF THE GROUND TRACKS. CONTOURS ARE AT 5 dB INTERVALS, AIRCRAFT TAKEOFF IS TO THE RIGHT FROM LOWER LEFT OF FIGURE AND ITS ALTITUDE IS OVER 8000 FT WHEN IT CROSSES THE AIRPORT. (REF. 3)

on both sides of the crossing flight path, the result of calculating the noise based on only the quiet high flying aircraft, rather than the sum of the noise contributions from both the initial takeoff segment and the crossing segment. Note that the contours would vanish entirely at the crossover point except for the smoothing provided by the grid contouring program.

Figure 5 illustrates large changes in noise values associated with a 180° turn shortly after takeoff. The principal anomaly is exhibited for grid positions inside the initial 90 degree turn and located towards the center of curvature for the turn. The anomaly consists of an apparent jump of several decibels (a maximum of 7 dB) from grid point to grid point. The major reason for the appearance of the anomaly is the abrupt transition from ground-to-ground attenuation to air-to-ground attenuation which occurs in this region. The abruptness of the transition near the center of the turn results from the large angular distance between radii through adjacent grid points. Thus, although the grid points may be only 1000 ft apart near the center, the aircraft position may have changed as much as 10,000 ft along the track, a distance sufficient in this example case to complete a transition from ground-to-ground attenuation to air-to-ground attenuation.

These results are also affected by the duration correction for positions inside the turn, the entering transition algorithm for this correction, and by the power reduction which occurs at about 70° through the turn.

There are a number of factors that must be considered in seeking a solution to these problems:

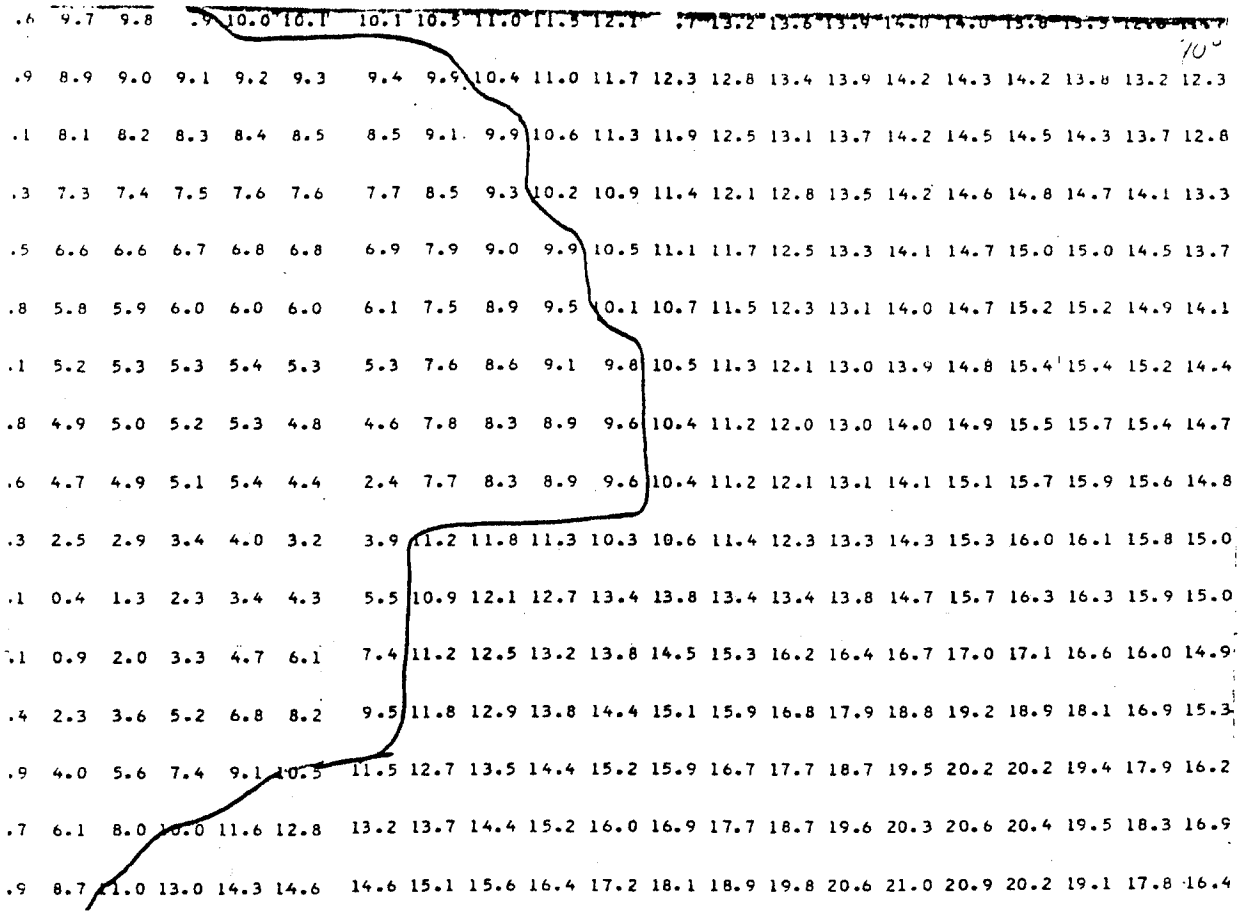

FIGURE 5: EXAMPLE OF RAPID CHANGES IN THE VALUES OF RELATIVE NOISE LEVELS BETWEEN ADJACENT GRID POINTS (1000 FT GRID) COMPUTED BY INM FOR AN AIRCRAFT TAKEOFF FROM THE LEFT OF THE FIGURE FOLLOWED BY A 180° LEFT HAND TURN. (REF. 4)

1. Discontinuities *must* be avoided in the gradient contour following program, or else the computer will find them and spend all its allowed time trying to find a point on the contour in the vicinity of a discontinuity.

2. The existing algorithms appear to strike a reasonable compromise with the ideal in treating many of the geometric situations in which there are a series of curved and straight segments. If the nearest segment methodology is retained in its basic form any solutions to the crossover problem should involve minimum changes in the existing algorithms. They have evolved by trial and error and appear to keep the program running relatively accurately in most situations. Clearly, an extensive change would have to be checked in many hypothethical situations to ensure that no *new* bugs appeared.

3. The basic noise data base in EPNL or SEL is ideally correct only for a straightline flyby, accounting for all the noise radiated to a point from the aircraft as it passes the observation point. The use of noise vs slant distance along a perpendicular to a segment implicitly assumes that the aircraft is on a straight path along the segment through the point nearest to the observation point. This assumption is essentially correct if the straight path is approximately six times the slant distance(s), centered on the nearest point. This assumption is violated if the aircraft changes power (noise output) while it is on the straight path, or if the aircraft turns so that the straight path is significantly shorter than six times the slant distance. If the observation point is outside of the turn, the noise

will be less than calculated. If it is on the inside of the turn, the noise will be greater, and the program provides a variable correction of plus 0 to 3 dB for observation points lying within the sector defined by the circular segment and its center.

An approach to this general problem was developed for NOISEMAP (Ref. 2). This program compares an integral of the noise of an aircraft that has an idealized directivity flying on the actual complex flight path with that of the same aircraft on a straight line path. The difference between the two values of the integral is then translated into a correction to the noise at the observation point.

Several alternative approaches were considered in attempting to solve the crossover wedge problem. These included choosing the nearest segment based on the three dimensional slant distance or its noise function. However, mixing three and two dimensional decision criteria renders the existing transition algorithms faulty in certain situations. Full use of three dimensional geometry, while retaining the nearest segment concept would require considerably more calculation particularly in the new algorithms required to ensure smooth transitions. The final result of this approach would probably be the elimination of one or more defined problems with the existing model, possible creation of new "bugs" which could hamper the revised program's operation, and the retention of other existing problems that were not explicitly addressed.

A more basic analysis of the fundamental nature of the methodological problems leads to recognition that the root of many of the observed problems lies in the concept of defining the

noise from an aircraft's overflight almost solely on its noise characteristics at its closest point of approach. Even if the program found the noisiest "closest point of approach" or the "closest point of approach of the path" instead of the closest point of the ground track, some problems would remain. Correction would still be required on both the inside and outside of turns for duration effects, and, in more complex geometry, provision would be required for the addition of noise from one or more segments, when it is significant.

In the present program, consideration is given to determining the existence of other segments that could contribute. However, the allowable region for considering the existence of a segment is sharply defined in its ground track geometry, (See Figs. 1 and 2). These sharp geometrical definitions of the range of influence of a ground track segment simplify the methodology, but also give rise to most of the potential discontinuities which then often require several complex calculations using the appropriate transition algorithms. They also serve to prevent the practical addition of the noise from a second segment to that of the nearest segment, except in narrowly defined transition regions.

A fundamental solution to these artificial constraints could be found if the noise contribution from a flight path segment to any arbitrary observation location were defined by an appropriate smoothly varying function. Then the contributions from all flight path segments of significance with respect to noise could be summed at an observation location to obtain the total noise energy (Sound Exposure Level or Effective Perceived Noise Level). Such a summation could automatically take care of duration effects associated with turns and contributions from multiple segments, almost as would an observer's ear. Further, it would not require any artificial algorithms to suppress artificially created discontinuities.

The function proposed for defining the noise from a straight segment of finite length is the 90° dipole representation of the directional characteristics of a typical aircraft in flight. Although this function is a much simplified approximation of the actual directivity of an aircraft, it appears to be a good estimator of the noise level time history of the sound measured near the ground for a straight line overflight as illustrated in Figure 6.

This function can also be applied to circular segments of flight paths when they are represented by a series of straight line segments. The proposed method for approximating a circular segment is to divide it into an even number of segments, not exceeding 30° per segment, such that the total length of the segments equals the circular arc length. The choice of a 30° sector limit reduces the maximum lateral error of the ground track to two percent of the radius of the circular segment.

Adoption of these proposed changes in fundamental methodology would substitute new subroutines for present subroutines, STRAIT and CURVE, and revise and simplify the subroutine HBT, eliminating its transition algorithms. A portion of subroutine EXPOSE could be modified to determine the noise-significant segments on a flight track for one or more flight profiles, and could be used to sum the noise contributions from the significant segments. The resulting program should have improved accuracy relative to the existing model in simulating the noise received on the ground from flight paths which involve turns.

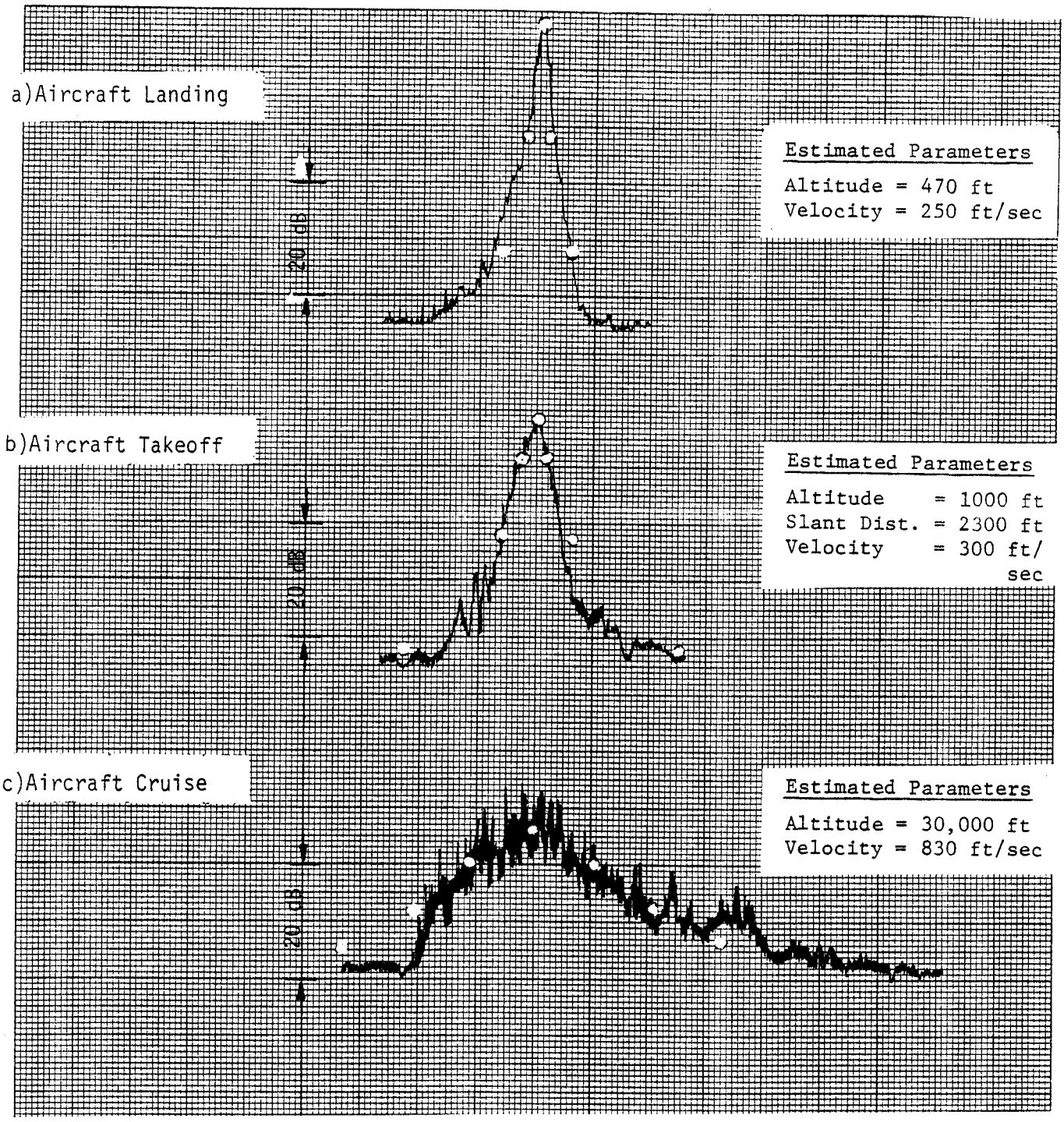

FIG. 6 THREE EXAMPLES OF AIRCRAFT FLYOVER A-WEIGHTED SOUND LEVEL TIME HISTORIES COMPARED WITH ESTIMATED 90° DIPOLE PROVING SOURCE RADIATION PATTERN PREDICTIONS WHICH ARE INDICATED BY OPEN CIRCLES.

4 DESCRIPTION OF NOISE AT START OF TAKEOFF ROLL

The ground roll portion of any departure is represented by a unique straight segment having special characteristics related to the airspeed and directionality of an aircraft at the start of takeoff. Of particular concern is the noise around the end of the segment when exposure levels are dominated or influenced by aircraft on this initial leg.

The INM computes exposure behind the aircraft at start of takeoff assuming it to be a nondirectional point source having a characteristic airspeed of 32 knots at the segment's end-point. For most airport noise analyses, this is an acceptable simplification since the levels behind the aircraft are often masked by noise from landings on the same runway or takeoffs in the opposite direction both of which are modelled more accurately. In some cases, however, where takeoffs are predominantly or totally on a single runway and landing noise is subordinate or ignored (as is the case in Figure 4), the resulting semicircular contours at the brake-release end of the runway significantly overstate the noise exposure.

Even with the improvement of the 90° dipole model, the true directional characteristics behind the aircraft are not adequately considered for this special situation. Thus, a more specialized approach must be utilized to improve predictions in the vicinity of this first segment. The model suggested here is based on empirical evidence collected during a measurement program of aircraft noise at the start of takeoff roll.

MEASUREMENTS

The measurements described in this section basically utilized an array of microphones positioned at various locations to the side and rear of aircraft as they accomplished engine runup, brake release, and takeoff. Runway 09 at Logan International Airport in Boston was selected for monitoring since it offers unobstructed views to aircraft on the runway for more than 1000 feet in a variety of directions. Additionally, monitoring periods were selected so that winds were generally less than 10 knots, weather was dry and no snow cover existed. Temperatures ranged from about 45° to 65°F. Specific measurement equipment is discussed in the Appendix.

The five measurement positions selected for monitoring are shown relative to the aircraft at start of takeoff in Fig. 7. The directivity pattern around each aircraft is assumed to be symmetrical about the longitudinal axis of the plane so that all five positions or their images can be used to define the variations in level in either of the rear quadrants (90° to 180° or 180° to 270°).

During the course of monitoring, a total of 48 aircraft were recorded, 23 of which were 727s, 15 of which were DC-9s and BAC 1-11s, and 6 of which were DC-10s and L-1011s. The remaining 4 consisted of a 707, a DC-8, a 747, and an A-300.

Analysis of Data

Sound exposure levels taken directly from the printout of portable noise monitors or reduced from analog recordings were identified for each aircraft type at each of the five measurement positions. Levels were normalized to 1000 ft. to correct

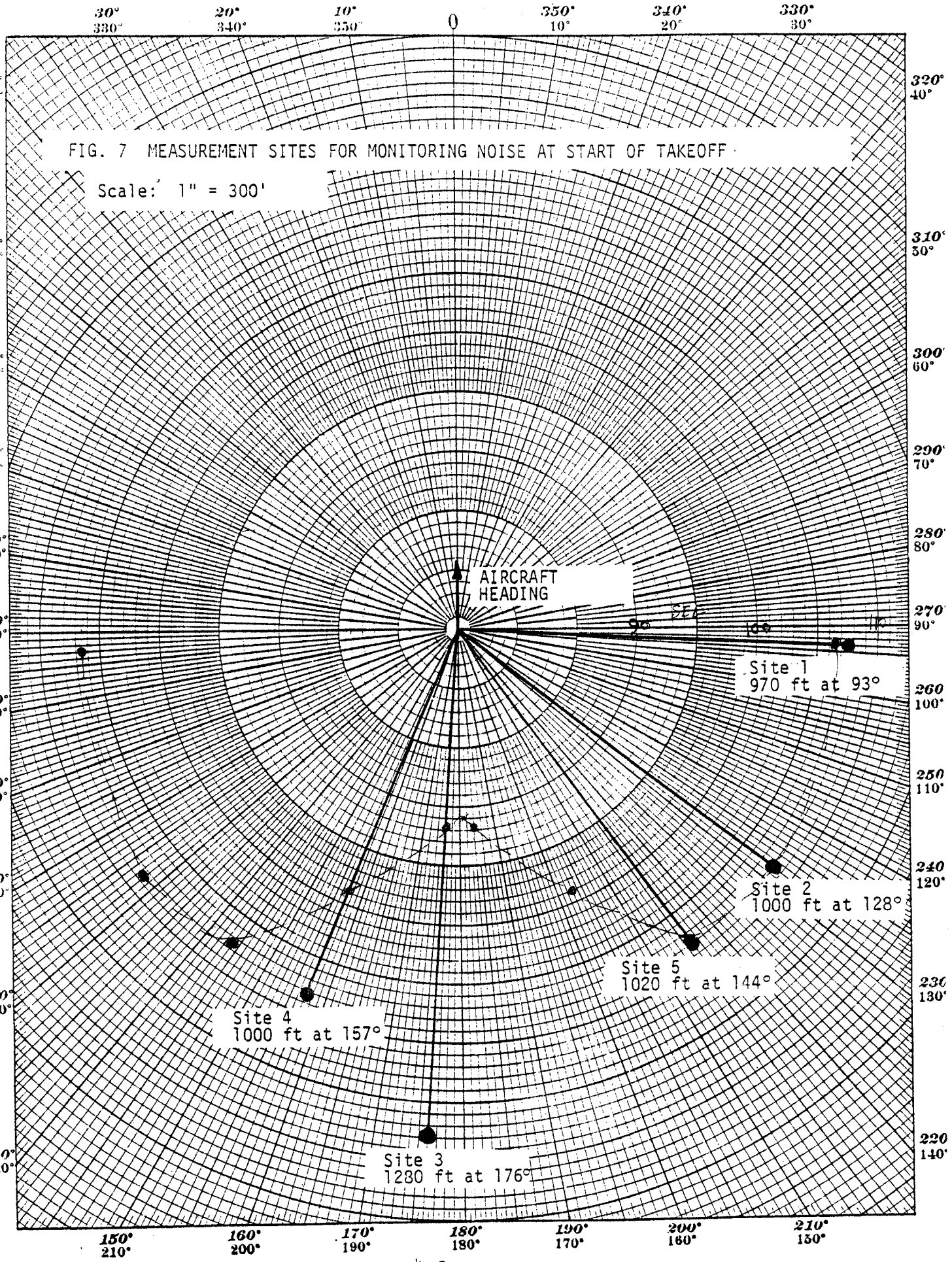

for small differences in distance to the runway, and then were used to compute energy average levels at each measurement angle for groups of similar aircraft. The results by location are summarized in Table 1 below.

Although certain aircraft types are not well represented in the measurements, especially at position 5, the energy averages of the data for the two most common types measured (the 2- and 3-engine narrow bodies) were defined within reasonable limits. Ninety percent confidence intervals for these sets of events ranged from ± 0.8 dB to ± 1.9 dB at sites 1 through 4, though up to ± 4.5 dB at site 5. Confidence intervals for the DC-10 and L-1011 data ranged from ± 1.6 dB to ± 3.7 dB at sites 1 through 4.

Considering the degree of accuracy with which levels of 2- and 3-engine narrow bodies can be identified, the fact that they constitute approximately 80% of all operations nationally, and that they will probably dominate noise exposure at most airports for the next twenty years, a fleet weighted average SEL was computed for each site to define a single curve most representative of levels at start of takeoff for the national mix of aircraft. The fleet weighted average, along with the averages for individual aircraft types, are plotted in Fig. 8 with curves drawn through the data points. Note from the curves of Fig. 8 that the levels for 707/DC-8 and 747 aircraft are less than those for the 2- and 3-engine narrow bodies, especially directly behind the aircraft. It is interesting to speculate that the difference is due, in part, to excess ground attenuation since the engines on those aircraft are mounted under the wing generally 3 to 5 feet above the ground while those on the DC-9 are 7 ft and those on the 727 either 10 or 12 ft above ground. The same phenomenon may also account for the fact that the DC-10/L-1011 data

TABLE 1: SUMMARY OF MEASUREMENT RESULTS

AIRCRAFT TYPE	Total No. of Events Recorded at Site 1	Energy Averaged SELs by Site (Normalized to 1000 Ft) 1 (93°)	2 (128°)	5 (144°)	4 (157°)	3 (176°)
4-Eng. low By-Pass Ratio, Narrow Body (707 and DC-8)	2	104.4	106.8	--	84.5	83.2
3-Eng. low By-Pass Ratio, Narrow Body (727)	23	107.4	109.8	108.0	100.0	92.3
2-Eng. low By-Pass Ratio, Narrow Body (DC-9 and BAC 1-11*)	15	107.7*	108.4*	104.8	101.4	91.7*
4-Eng. High By-Pass Ratio Wide Body (747)	1	104.8	96.3	--	87.3	81.9
3-Eng. High By-Pass Ratio, Wide Body (DC-10 and L-1011	6	101.5	104.2	--	98.2	95.0
2-Eng. High By-Pass Ratio, Wide Body (A-300)	1	96.6	96.0	--	--	--
Fleet Weighted Average SEL		106.5	108.5	107.5	99.0	91.8
Fleet Weighted Average SEL Relative to that at Site 1		0	+2.0	+1.0	-7.5	-14.7

*Exclusion of the BAC 1-11 from the Energy Averaged SELs for 2-eng. narrow bodies, at Sites 1, 2 and 3 reduces those averages by 0.2, 0.3, and 0.1 dB, respectively.

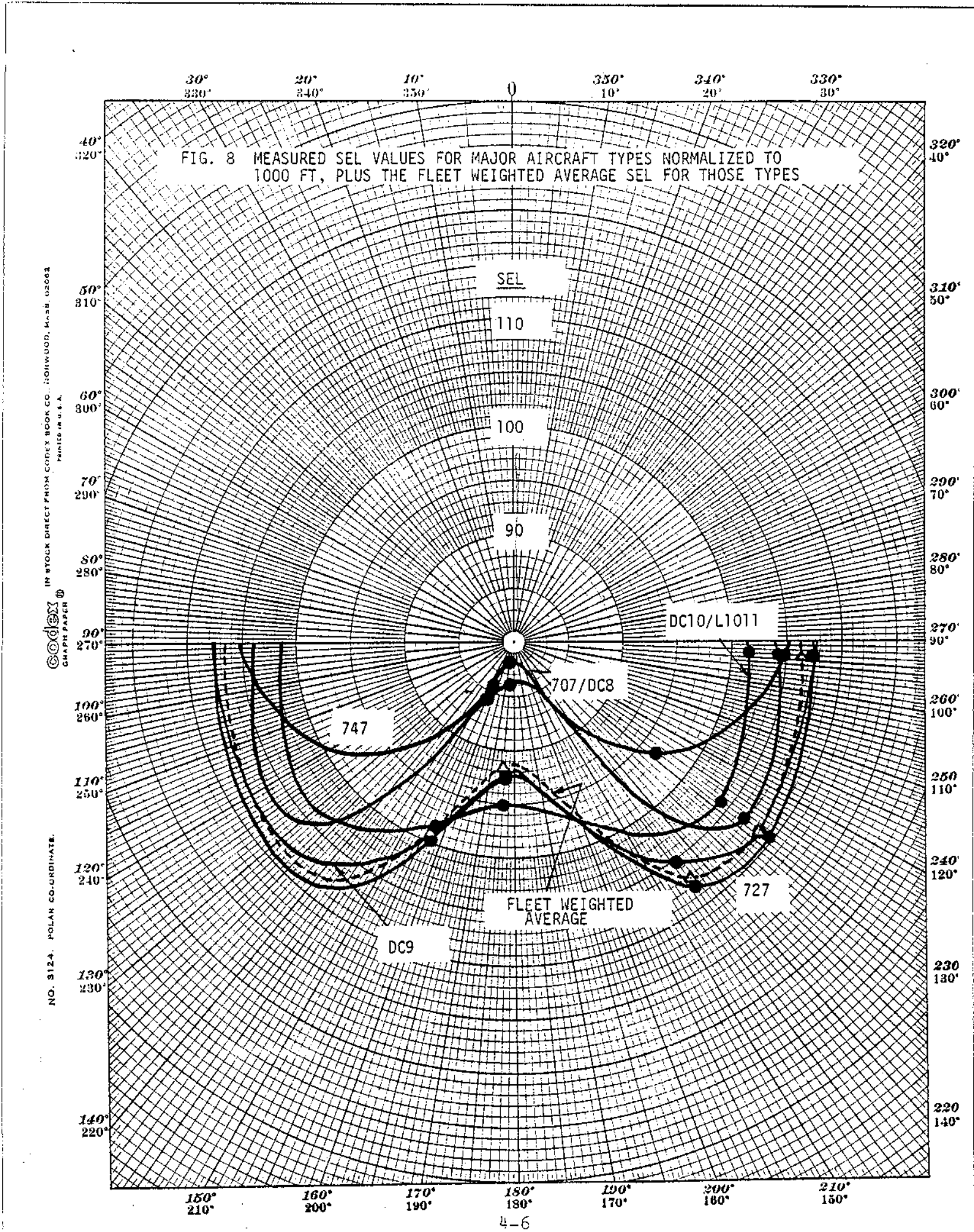

are the highest of any aircraft directly behind the plane. Exhausts of their middle engines are 30 and 16 feet above the ground, respectively. [5] Future refinements of the INM might address these differences, however, the present fleet with its dominance of DC-9s and 727s does not appear to warrant the additional computations associated with aircraft type specific noise definitions.

In addition to the SELs for each aircraft, Effective Perceivied Noise Levels (EPNLs) were computed for the 44 operations recorded on analog tape during the two monitoring periods. The recordings were made only at Sites 1, 2, and 5 (93°, 128°, and 144° off the aircraft heading) and not all events were recorded at each site, but the data were used to determine whether the differences between EPNL and SEL changed with angle to the aircraft.

For the 2- and 3-engine narrow bodies, the difference between EPNL and SEL does, in fact, increase slightly at least through 144°. Table 2 below summarizes the observed changes. Insufficient data were available to draw similar conclusions for other aircraft types.

TABLE 2: MEASURED DIFFERENCES BETWEEN EPNL AND SEL WITH CHANGE IN ANGLE TO THE AIRCRAFT

AIRCRAFT TYPE	EPNL-SEL (in dB)		
	Site 1 (93°)	Site 2 (128°)	Site 5 (144°)
3-eng. Narrow Body	3.7	4.3	4.7
2-eng. Narrow Body	3.8	4.5	5.6
Fleet Weighted Avg.	3.7	4.3	4.8

The average increase in the difference between the two measures relative to their difference at 93° (nominally 90°) is 0.6 dB at 128° and 1.1 dB at 144°. Rationalizing that the relative difference will eventually decrease back to 0 at some point behind the aircraft where levels are lowest and pure tones are less pronounced, one can visualize curves of EPNL for 2- and 3-engine narrow bodies similar in shape to those in Fig. 8, but differing slightly in relative value.

Considering that the differences between the EPNL and SEL curves would vary, for the most part, by less than 1 dB, that fewer events were used to determine the EPNL values, and that fewer aircraft types are represented in the measurement data, it is suggested that only the curve for relative SEL values be modeled and that those corrections then be applied to whichever metric is being used by the program.

Application of the data presented here to a revised model for start of takeoff is summarized in the section on "Recommendations."

5. RECOMMENDATIONS

The analysis made of various anomalies in the INM leads to recommending a change in its fundamental methodology, to make it a more accurate simulation of the noise from aircraft on flight paths that include turns. The fundamental change is to allow the model to hear at each observation location the noise that is radiated by the aircraft flight on each of its flight path segments, retaining and summing the noise for all segments that are significant within a predetermined error to the energy sum. This change eliminates the present method of defining the total noise of an aircraft flight as that defined by the closest point of approach on the ground track. Further, this change eliminates several transition algorithms required with the present methodology to avoid discontinuities in the computed observer noise function, and the algorithms that attempt to approximate the increase of noise duration for observers located inside turns.

The principal changes required in program logic involve describing circular segments by an even number of straight segments and defining the entire noise field from any straight segment. These changes add a subroutine, probably in the preprocessor, to define the segments that approximate each turn and renumber the track segments; replace subroutines STRAIT and CURVE with a new Straight Segment Noise; modify HBT to delete unnecessary transition algorithms and interface properly between Straight Segment and EXPOSE; and modify slightly EXPOSE to determine noise significant segments and the total noise for each flight on all significant segments. Additionally, a change is proposed to more accurately describe the noise behind an aircraft at the start of takeoff roll.

These changes are described in the following subsections:

- Circular Segment Approximation by Straight Segments
- Straight Segment Noise
- Takeoff Roll Segment Noise.

Each subsection describes its purpose, defines the appropriate geometry and derives necessary relationships, and outlines the new calculations to be performed in the computer.

Circular Segment Approximation by Straight Segments

Any circular portion of a ground track is replaced by an even number of straight line segments, selected so that the sum of the segment lengths equals the arc length of the track and so that no segment exceeds an angle of 30°. This latter constraint limits the position error to a maximum of 0.02 times the radius of the track, or 180 ft for a typical radius of 9000 ft. See Figure 2 for examples.

Geometrical Relationships for a Straight Segment Approximation

The principal geometrical elements are defined in Figure 9:

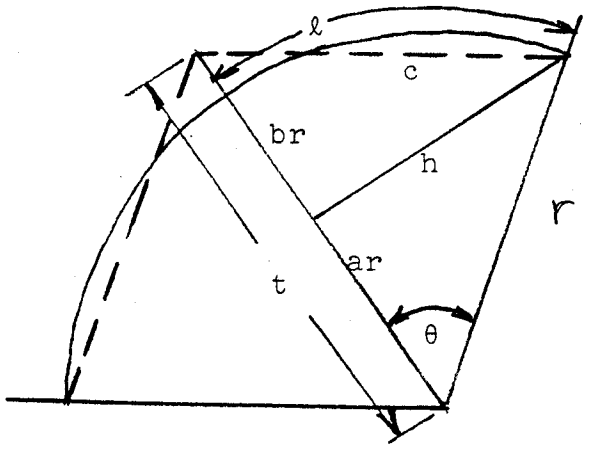

FIGURE 9: SKETCH OF APPROXIMATION OF CIRCULAR ARC BY STRAIGHT LINE SEGMENTS.

The following define the relationships amongst the geometrical elements:

$$h = r \sin \theta$$

$$a = \cos \theta$$

$$\ell = r\,\theta \text{ where } \theta \text{ is in radians}$$

$$c = [h^2 + (br)^2]^{\frac{1}{2}} .$$

Let $c = \ell$, i.e., straight segment length equals arc lenth.

$$\therefore r\theta = [r^2\sin^2\theta + b^2r^2]^{\frac{1}{2}}$$

$$\therefore b = \sqrt{\theta^2 - \sin^2\theta}$$

and $t = r(\cos \theta + \sqrt{\theta^2 - \sin^2\theta^2})$.

The following examples show the value of t/r for selected values of θ. The lateral error from the actual circular arc is given by (t/r - 1).

θ(°)	b	a	t/r	Lateral Fractional Error
22.5°	.09	.92	1.01	0.01
30°	.16	.87	1.02	0.02
45°	.34	.71	1.05	0.05
60°	.59	.50	1.09	0.09

Figure 10 illustrates three examples of these approximations:

- 90° arc approximated by 2 segments (45°/segment)
- 90° arc approximated by 4 segments (22½°/segment)
- 60° arc approximated by 2 segments (30°/segment)

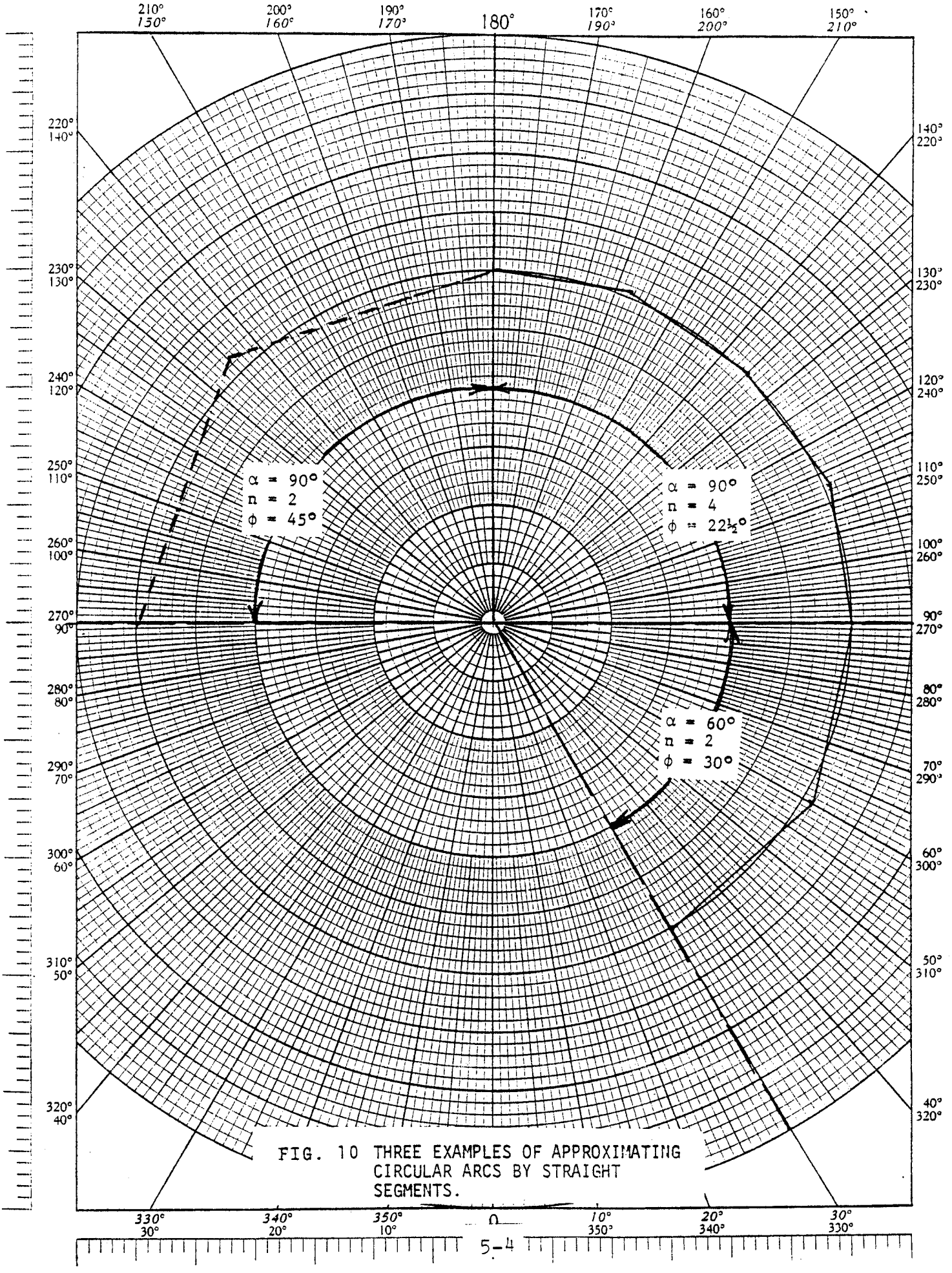

FIG. 10 THREE EXAMPLES OF APPROXIMATING CIRCULAR ARCS BY STRAIGHT SEGMENTS.

The calculation procedure assumes a choice of limiting the maximum lateral error to two percent (i.e., 30°/segment). This choice leads to 2 segments for arcs of up to 60°, 4 segments for arcs of 60-120°, 6 segments for arcs of 120-180°, etc.

Calculations

The calculations are to be performed in a preprocessor, and the track segments renumbered accordingly. The calculations are:

1. Select an even number N such that when the arc angle (α) is divided by N the resulting angle (θ) is equal to or less than 30°:

   Define: $m = \frac{\alpha}{60}$ and round up to nearest integer.

2. Define: $N = 2m$.

3. Define: $\theta = \frac{\alpha}{2m}$.

4. Define coordinates of start of first segment:

   $$P_1(x) = P_0(x) + r \cos \tau$$

   $$P_1(y) = P_0(y) + r \sin \tau$$

   $$P_1(z) =$$

5. Determine the distance (t) from the center of the circular arc (P_0) to the start of the even numbered segments.

   $$t = r(\cos \theta + \sqrt{\theta^2 - \sin^2\theta}) .$$

6. Determine coordinates of start of second segment:

   $$P_2(x) = P_0(x) + t \cos(\tau + \theta)$$

   $$P_2(y) = P_0(y) + t \sin(\tau + \theta)$$

   $$P_2(z)$$

Straight Segment Noise

A straight segment is defined by the position of the start of the segment (P_1), a unit vector ($\hat{r}$) along the segment, and the segment's length (ℓ). The position of an observation point (P) relative to the straight segment is defined by the slant distance (S) along the perpendicular from the observation point to the straight segment or its extension, and the distance (q_1) along the segment, or its extension, from the start of the segment to the position of its intersection with the perpendicular through P.

The operating parameters for the aircraft (velocity and thrust) are determined by the distance, q_1 (See Fig. 11.) If q_1 is negative, the operating parameters are those associated with the start of the segment (P_1). If q_1 is larger than ℓ (the length of the segment) the operating parameters are those associated with the end of the segment (P_2). If q_1 lies between 0 and ℓ the operating parameters are those associated with the position on the segment defined by q_1.

The noise energy attributed to an aircraft flying on the segment is determined by the noise fraction (F) times the noise energy for the aircraft flying on an infinite straight line path extension of the straight segment. The noise fraction is calculated using an approximation of the 90° dipole model for the aircraft's directional radiation pattern.

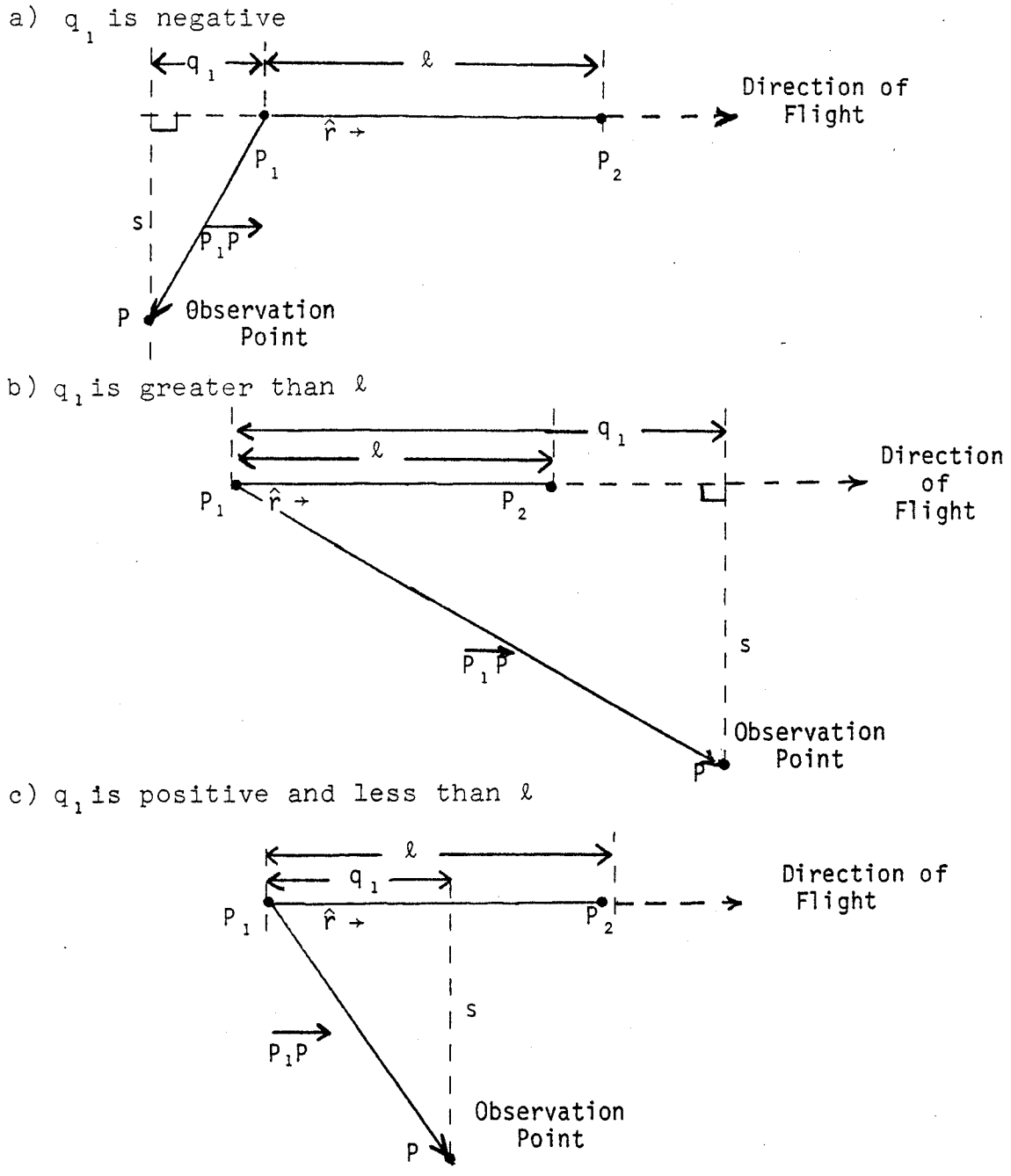

FIG. 11 ILLUSTRATION OF THE THREE RELATIVE POSITIONS OF AN OBSERVATION POINT AND A STRAIGHT SEGMENT.

Derivation of Fractional Sound Exposure

The sound exposure level defined in the INM is that for a straight line path of infinite length. For finite straight segments the sound exposure level is less than that associated with an infinite straight path. The sound exposure fraction for a straight line segment is defined as the sound exposure at an observation position attributed to an aircraft's flight on a finite straight segment divided by the sound exposure that would be observed at the position if the straight segment had infinite length. The following derivation is based on the 90° dipole model for the time history of the sound received at an observation position from an aircraft flyby on a straight segment of infinite length.

The geometry utilized in this derivation is illustrated in the sketch below:

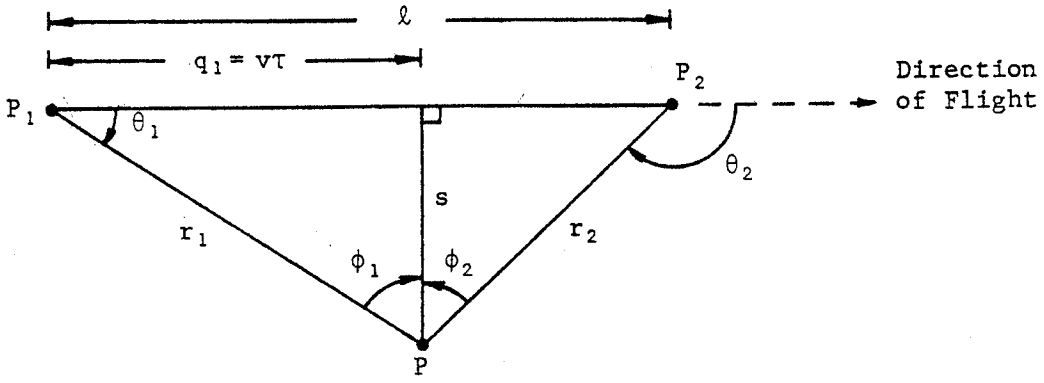

Here, by convention, θ is the angle between the direction of flight and the direction from the aircraft to the observer. It varies from 0° to 180° or 0 to π radians. ϕ is the angle between the observer and the aircraft and the perpendicular through the observer to the direction of flight. For ϕ and θ in degrees, $\phi = 90° - \theta$ so that ϕ ranges from 90° to -90°. It is positive when the aircraft is approaching the observer and negative when the aircraft has passed.

For the 90° dipole the ratio of the mean square sound pressure at P from the aircraft at distance r to that received when the aircraft is at the closest distance s is given by:

$$\frac{p_r^2}{p_s^2} = \sin^4\theta \ . \qquad (1)$$

The total sound exposure (β) is the integral of the mean square sound pressure over time (τ). Between two points, P_1 and P_2,

$$\beta_{12} = \int_{t_1}^{t_2} p_r^2 dt \qquad (2)$$

From the geometry, letting $t = \tau$

$$\tau = \frac{s}{v} \cot\theta$$

and

$$d\tau = \frac{-s\, d\theta}{v \sin^2\theta} \quad . \qquad (3)$$

Combining (1) through (3) the sound exposure between positions θ_1 and θ_2 is

$$\beta_{12} = -p_s^2 \frac{s}{v} \int_{\theta_1}^{\theta_2} \sin^2\theta d\theta$$

$$= -p_s{}^2 \frac{s}{v} \left| \frac{\theta}{2} - \frac{\sin 2\theta}{4} \right|_{\theta_1}^{\theta_2}$$

$$= -p_s{}^2 \frac{s}{2v} [\theta_2 - \theta_1 + \sin(\theta_1 - \theta_2)\cos(\theta_1 + \theta_2)] \quad . \quad (4)$$

Over an infinitely long segment, θ varies from 0 to π radians, and from equation (4), the resulting sound exposure (β_{INF}) is:

$$\beta_{INF} = -\pi \frac{p_s{}^2 s}{2v} \quad . \tag{5}$$

It then follows that the fractional sound exposure (F_{12}) associated with a straight segment of finite length extending between θ_1 and θ_2 (θ in radians) is:

$$F_{12} = \frac{1}{\pi} [\theta_2 - \theta_1 + \sin(\theta_1 - \theta_2)\cos(\theta_1 + \theta_2)] \tag{6}$$

To avoid the computations of θ_1 and θ_2 in the INM, two alternative approximations are proposed for Equation (6). They are of the general form:

$$g = \frac{\sin\phi}{2}$$

and

$$h = A\sin\phi\left(1 - \frac{B}{A}|\sin\phi|\right) \quad .$$

In their explicit forms, g_{12} and h_{12} represent the sums or differences of two functions, g_1 and g_2 or h_1 and h_2, respectively, where g_n and h_n are approximations of the noise fractions of segments extending between points p_n and the intersection of the perpendicular to the direction of flight through the observation point P. Specifically,

$$g_1 = \frac{\sin\phi_1}{2}$$

$$g_2 = -\frac{\sin\phi_2}{2}$$

$$g_{12} = \left|g_1 + g_2\right| = \left|\frac{\sin\phi_1}{2} - \frac{\sin\phi_2}{2}\right|$$

$$= \left|\frac{q_1}{2r_1} - \frac{(q_1 - \ell)}{2r_2}\right| \quad , \tag{7}$$

and

$$h_1 = .65 \sin\phi_1 \, (1 - .231|\sin\phi_1|)$$

$$h_2 = -.65 \sin\phi_2 \, (1 - .231|\sin\phi_2|)$$

$$\begin{aligned} h_{12} &= |h_1 + h_2| \\ &= \left|.65 \sin\phi_1(1 - .231|\sin\phi_1|) - .65 \sin\phi_2(1 - .231|\sin\phi_2|)\right| \\ &= \left|\frac{.65q_1}{r_1}\left(1- .231\left|\frac{q_1}{r_1}\right|\right) - \frac{.65(q_1-\ell)}{r_2}\left(1-.231\left|\frac{q_1-\ell}{r_2}\right|\right)\right| \\ &= \left|\left(\frac{.65q_1}{r_1} - \frac{.15q_1}{r_1}\left|\frac{q_1}{r_1}\right|\right) - \left(\frac{.65q_2}{r_2} - \frac{.15(q_1-\ell)}{r_2}\left|\frac{q_1-\ell}{r_2}\right|\right)\right| \end{aligned} \tag{8}$$

The following table compares the values F, g, and h for various values of ϕ and θ. Note that although h is more complex than g, it is a more accurate estimator of F.

TABLE 3 A COMPARISON OF FUNCTIONS F, g, AND h FOR COMPUTING FRACTIONAL SOUND EXPOSURE FROM A STRAIGHT SEGMENT.
(all angles in degrees)

					Approximation g		Approximation h	
ϕ_1	ϕ_2	θ_1	θ_2	F_{12}	g_{12}	Error $(g_{12}-F_{12})$	h_{12}	Error $(h_{12}-F_{12})$
45	45	45	45	0.000	0.000	0	0.000	0
0	0	90	90	0.000	0.000	0	0.000	0
					(F, g, and h are also 0 for any other $\phi_1 = \phi_2$ or $\theta_1 = \theta_2$)			
90°	75	0°	15°	.004	.017	.013	.012	.008
	60		30	.029	.067	.038	.050	.021
	45		45	.091	.146	.056	.115	.024
	30		60	.196	.250	.054	.213	.017
	0		90	.500	.500	0	.500	0
	-30		120	.804	.750	-.054	.788	-.017
	-45		135	.909	.854	-.056	.885	-.024
	-60		150	.971	.933	-.038	.950	-.021
	-75		165	.996	.983	-.013	.988	-.008
	-90		180	1.000	1.000	0	1.000	0
75°	60	15°	30	.025	.050	.025	.037	.012
	45		45	.087	.129	.042	.103	.016
	30		60	.192	.233	.041	.200	.008
	0		90	.496	.483	-.013	.488	-.008
	-30		120	.801	.733	-.068	.775	-.026
	-45		135	.905	.837	-.068	.873	-.032
	-60		150	.967	.916	-.051	.938	-.029
	-75		165	.992	.966	-.026	.976	-.016
	-90		180	.996	.983	-.013	.988	-.008
60°	45	30°	45	.062	.079	.017	.066	.004
	30		60	.167	.183	.016	.163	-.004
	0		90	.471	.433	-.038	.450	-.021
	-30		120	.776	.683	-.093	.738	-.038
	-45		135	.880	.787	-.093	.835	-.045
	-60		150	.942	.866	-.076	.901	-.041
	-75		165	.967	.916	-.051	.938	-.029
	-90		180	.971	.933	-.038	.950	.017
45°	30	45°	60	.105	.104	-.001	.097	-.008
	0		90	.409	.354	-.055	.385	-.024
	-30		120	.714	.604	-.110	.672	-.042
	-45		135	.818	.707	-.111	.769	-.049
	-60		150	.880	.787	-.093	.835	-.045
	-75		165	.905	.837	-.068	.873	-.032
	-90		180	.909	.854	-.055	.885	-.024
30°	0	60°	90	.304	.250	-.054	.288	-.017
	-30		120	.609	.500	-.109	.575	-.034
	-45		135	.714	.604	-.110	.672	-.042
	-60		150	.776	.683	-.093	.738	-.038
	-75		165	.801	.733	-.068	.775	-.026
	-90		180	.804	.750	-.054	.788	-.017

Calculations

The calculations performed are:

1. Define (q_n) the distance from P_n to the intersection of the perpendicular from P to the segment or its extension. That is,

$$q_1 = \overrightarrow{P_1P} \cdot \hat{r} \quad \text{and} \quad q_2 = \overrightarrow{P_2P} \cdot \hat{r} = q_1 - \ell$$

2. Define (s) the slant distance from P to the segment or its extension:

$$s = \sqrt{|\overrightarrow{P_nP}|^2 - q_n^2}$$

3. Compute the noise fraction (F_{12}) by algebraically summing the noise fractions (F_1) and (F_2) between the perpendicular and P_1 and P_2, respectively, then taking the absolute value of the sum.

for approximation (g)	for approximation (h)
$F_1 \doteq \frac{q_1}{2\lvert\overrightarrow{P_1P}\rvert}$	$F_1' \doteq 1.30F_1(1 - .462\lvert F_1\rvert)$
$F_2 \doteq -\frac{(q_1 - \ell)}{2\lvert\overrightarrow{P_1P} - \ell\hat{r}\rvert}$	$F_2' \doteq -1.30F_2(1 - .462\lvert F_2\rvert)$
$F_{12} \doteq \lvert F_1 + F_2\rvert$	$F_{12}' \doteq \lvert F_1' + F_2'\rvert$

4. Define X, the distance along the segment from P_1 at which the aircraft is located for the purpose of defining its operational parameters as follows:

   If $q < 0$, $X = 0$
   If $q > \ell$, $X = \ell$
   If $0 < q < \ell$, $X = q$

5. Return S, a and X to calling subroutine.

Takeoff Roll Segment Noise

The takeoff roll segment represents a special case of the general model for straight segments. In considering the noise behind the aircraft at start of takeoff, the model is dealing only with the first segment of a flight track and points behind the aircraft where q_1 is negative and θ_1 is > 90°. A variation of Fig. 11(a) picturing the geometry applicable to this special case is reproduced below:

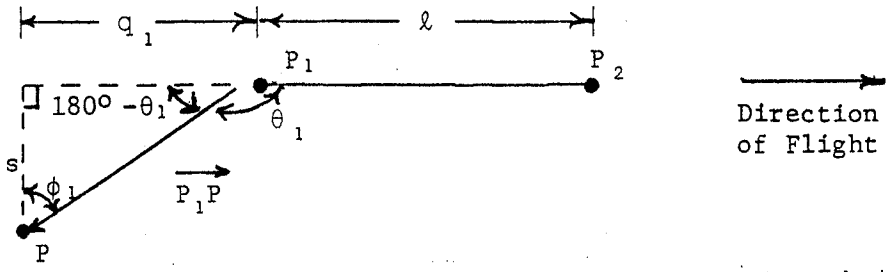

Before deriving a function for modeling the noise at point P, a check of the measured data was made against the new INM noise data base to consider the validity of the 32 knot minimum airspeed associated with point P_1 since that value clearly influences the level at point P.

Determination of Minimum Segment Airspeed

Takeoff SELs for 2- and 3-engine narrow bodies and 3-engine wide bodies were computed from the new data base for a 1000 ft slant distance using the INM's existing algorithms for excess ground attenuation, shielding, and adjustments for airspeed. These levels were then adjusted downward by 3 dB in accordance with the function F_{12} described in the previous subsection so as to model a straight segment for a nearby observer opposite the start of takeoff roll ($q_1 = 0$). The computed levels were then compared to the measured levels at Site 1 (nominally 90° to the aircraft, with q_1 again equal to 0). Results of the comparisons showed that

computed and measured SELs were within 2.6 dB of each other for 727s. For DC-9s and 737s, the computed and measured levels were 5.1 dB apart, and for DC-10s and L-1011s the levels were 8.6 dB apart. In all cases, the measured levels were highest.

The fleet weighted average of these differences results in a 3.1 dB underestimate of the measured data. Although multiple factors could be contributing to this difference, one consideration is the reasonableness of the airspeed adjustment given the 32 knot minimum for the initial point of the takeoff roll segment. Much better correlation between computed and measured levels would, in fact, occur if the minimum airspeed for the initial segment were lowered to 16 knots in the revised model. Such a change would be consistent with the logic used to define the fractional sound exposure for the initial segment and would bring estimated and measured SELs to within 0.1 dB of each other on a fleet weighted basis.

Assuming this adustment is made, it then is possible to compute the levels at points behind the aircraft relative to a level computed at a point to the side of the aircraft. For this reason, the fleet weighted average Sound Exposure Levels of Fig. 8 have been translated into relative levels as a function of angle in Fig. 12. It remains necessary to develop a mathematical expression to approximate the adjustments suggested by this curve.

Determination of Relative Levels for $q_1 < 0$, $\theta_1 > 90^o$

Because the INM does not actually compute θ and because it works with antilogs (energy) rather than logarithms (decibels) in determining the noise from a given segment, it is useful to redraw the curve of Fig. 12 transforming the axes into relative energy (energy relative to that at 90° to the aircraft) and the cosine of the angle (θ_1) between the aircraft heading and the

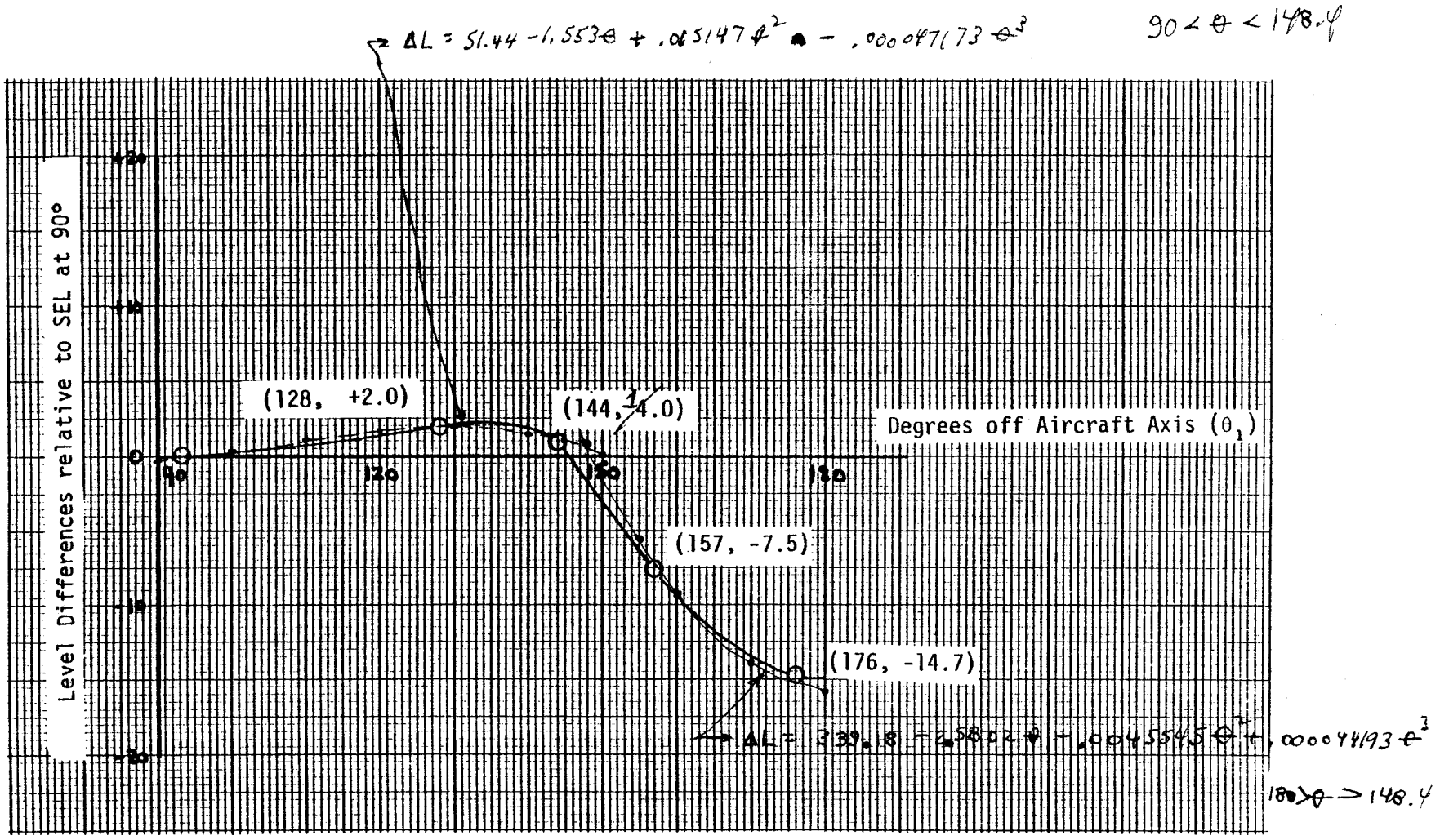

FIG. 12 LEVELS RELATIVE TO SEL AT 90° AS A FUNCTION OF ANGLE TO THE AIRCRAFT AT START OF TAKEOFF FOR THE FLEET WEIGHTED AVERAGE AIRCRAFT.

vector $\overrightarrow{P_1P}$. This curve is depicted in Fig. 13. Given a mathematical expression for the curve and the fact that:

$$\cos(\theta_1) = -\cos(180° - \theta_1) = \frac{q_1}{|\overrightarrow{P_1P}|} \text{ for } q_1 < 0 \ ,$$

the energy at any angle behind the aircraft can be related to the energy at 90° to the aircraft in terms of quantities already known within the INM.

Although many forms of general functions were tested for their suitability, no single simple expression could be identified that approximated the curve with an accuracy of 2 dB or less. Instead, two functions (both 3rd order polynomials) were identified, one approximating the curve when $\cos(\theta_1) \geq -.76889$, and one approximating the curve when $\cos(\theta_1) < -.76889$. The two functions are given below:

- for $0 > x = \cos(\theta_1) \geq -.76889$ (i.e. $90° < \theta_1 \leq 140.2543°$)

$$y = 6.7414\ x^3 + 7.7667\ x^2 + 1.2771\ x + 1.0000 \qquad (9)$$

- for $x = \cos(\theta_1) < -.76889$ (i.e. $180° \geq \theta_1 > 140.2543°$)

$$y = 47.2857\ x^3 + 159.3146\ x^2 + 176.7059\ x + 64.7214 \qquad (10)$$

Equations (9) and (10) are also plotted in Fig. 13 to show the closeness of fit between these approximations and the desired curve through the data.

Converting y to a relative decibel level using the function

$$y' = 10 \log(y) \qquad (3)$$

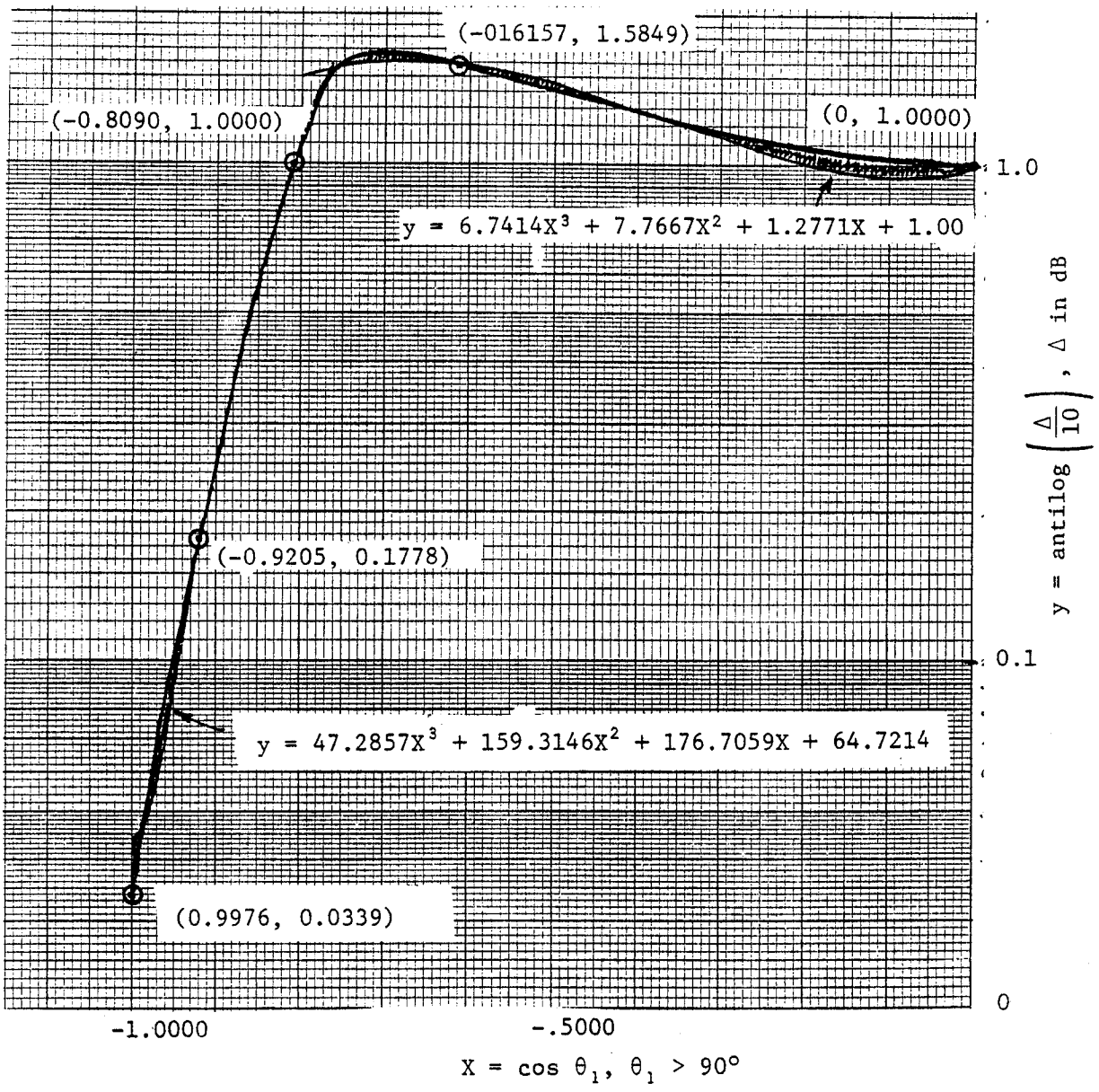

FIG. 13 RELATIVE ENERGY (Re ENERGY AT 90° TO AIRCRAFT) AS A FUNCTION OF COS (θ_1).

and comparing values of y' against the curve in Fig. 12 yields, for any $90° < \theta_1 \leq 170°$, a maximum error of about 0.3 dB. This occurs at an angle of $\theta = 100°$. For any $170° < \theta_1 \leq 180°$ an error as high as 1.1 dB occurs when $\theta = 180°$ directly behind the aircraft.

Calculations

The calculations to be performed by the program are as follows: *

1. Determine whether $\overrightarrow{P_1P_2}$ is the first segment of a flight track.
2. If true, determine that q_1 is negative.
3. If true, determine the distance $|\overrightarrow{P_1P}|$ from the aircraft to the observer.
4. Define a new point P_0 at slant distance $s_0 = |\overrightarrow{P_1P}|$ such that P_0 is on the perpendicular to $\overrightarrow{P_1P_2}$ through P_1 (i.e., $q_1 = 0$).
5. Compute the noise fraction (F_{12} or F'_{12} depending on the approximation used in the straight segment calculations) for the point P_0 and the segment $\overrightarrow{P_1P_2}$.
6. Compute $x = \dfrac{q_1}{|\overrightarrow{P_1P}|}$.
7. Compute y as a function of x using the appropriate relationship defined by equation (9) or (10) above depending on the value of x.
8. Compute a new F_{12} or F'_{12} (for point P) as the product of y and F_{12} or F'_{12} (for point P_0). The resultant noise fraction, when applied to the energy for an infinite line will adjust the value for the combined effect of the segment length and the directivity pattern to the rear of the aircraft.

*In addition, change the minimum aircraft velocity, applicable at P_1, from 32 to 16 knots.

REFERENCES

1. Wyle Laboratories, "Programmer's Manual for the Integrated Noise Model (Vol. 1)," Wyle Research Report WCR 77-7, Prepared for U.S. Department of Transportation, Contract No. DOT-OS-50256.)

2. Galloway, William J., "Community Noise Exposure Resulting from Aircraft Operations: Technical Review," Aerospace Medical Research Laboratory, Wright-Patterson Air Force Base, Ohio, AMRL-TR-73-106.

3. U.S. DOT, Transportation Systems Center, Communication reporting run of crossover case, 22 February 1980.

4. U.S. DOT, Transportation Systems Center, Communication reporting grid test case with turn after takeoff, February 1980.

5. FAA Advisory Circular 150/5325-5B, "Aircraft Data," 30 July 1975.

APPENDIX A

MEASUREMENT EQUIPMENT

Recording equipment at each of the monitoring locations generally consisted of a Kudelski Nagra IV-SJ two-channel tape recorder and/or a BBN Type 614 Portable Noise Monitor. The rationale for utilizing different instrumentation from one site to another was twofold. It permitted simultaneous collection of data at more sites than would have been possible with only a single version of the instrumentation system, and secondly, use of the 614s in particular minimized the amount of data reduction necessary in the analysis. An itemization of specific equipment used during the monitoring program is given in Table A-1.

TABLE A-1 MEASUREMENT INSTRUMENTATION

Equipment Type (No.)	Manufacturer	Type	Serial Number	Location Used
Portable Noise Monitors (4)	BBN	614	790703	Site 1, 20 Feb
			772527	Site 2, 20 Feb
			772528	Site 3, 20 Feb
			773110	Site 4, 20 Feb
Stereo Tape Recorders (3)	Kudelski	NAGRA IV-SJ	2093	Site 1, 20 Feb
				Site 2, 23 Jun
				Site 5, 23 Jun
			7724	Site 1, 23 Jun
1 in.Condenser Microphones (4)	Bruel & Kjaer	4131	43943	Site 1, 20 Feb & 23 Jun
			123467	Site 2, 20 Feb
				Site 5, 23 Jun
			179425	Site 3, 20 Feb
			97865	Site 4, 20 Feb
				Site 2, 23 Jun
Preamplifiers (6)	Gen Rad	1560-P42	1969	Site 1, 20 Feb
				Site 5, 23 Jun
			2055	Site 2, 20 Feb
			3860	Site 3, 20 Feb
			3853	Site 4, 20 Feb
			3829	Site 1, 23 Jun
			4111	Site 2, 23 Jun
Power Supplies (4)	BBN	--	--	One per Site
Pistonphones (3)	Bruel & Kjaer	4220	169818	All sites, 20 Feb
			668447	All Sites, 23 Jun